

# Acoustic energy harvesting with irradiated cross-linked polypropylene piezoelectret films

Yuan Xue<sup>1</sup> , Jinfeng Zhao<sup>2,5</sup> , Xiaoqing Zhang<sup>1,5</sup>,  
Gerhard M Sessler<sup>3</sup>  and Mario Kupnik<sup>4</sup>

<sup>1</sup> Shanghai Key Laboratory of Special Artificial Microstructure Materials and Technology, School of Physics Science and Engineering, Tongji University, 1239 Siping Road, 200092 Shanghai, People's Republic of China

<sup>2</sup> School of Aerospace Engineering and Applied Mechanics, Tongji University, 100 Zhangwu Road, 200092 Shanghai, People's Republic of China

<sup>3</sup> Institute for Telecommunications Technology, Technische Universität Darmstadt, Merckstrasse 25, D-64283 Darmstadt, Germany

<sup>4</sup> Measurement and Sensor Technology Group, Technische Universität Darmstadt, Merckstrasse 25, D-64283 Darmstadt, Germany

E-mail: [jinfeng.zhao@tongji.edu.cn](mailto:jinfeng.zhao@tongji.edu.cn) and [x.zhang@tongji.edu.cn](mailto:x.zhang@tongji.edu.cn)

Received 24 October 2018, revised 19 January 2019

Accepted for publication 22 January 2019

Published 11 June 2019



CrossMark

## Abstract

Piezoelectret films prepared by irradiated cross-linked polypropylene (IXPP) not only feature a large figure of merit ( $d_{33} \cdot g_{33}$ , FoM) and a nearly flat response of the sensitivity as a microphone ( $4 \text{ mV Pa}^{-1}$ ) in the audio range, but also exhibit a good impedance match to air. Therefore, this material is appropriate for air-coupled sonic and ultrasonic applications. In this work, we report acoustic energy harvesting using IXPP piezoelectret films without mass loading both in ultrasonic and low-frequency ranges. Under an input sound pressure level (SPL) of 100 dB (or 2 Pa) and a resonance frequency of 53 kHz, a maximum output power of 7.2 nW is obtained for an IXPP film harvester. Despite its high resonance frequency, the large FoM of IXPP piezoelectret films suggests itself to be a promising candidate also for low-frequency acoustic energy harvesting with the help of Helmholtz resonators. An output power of 10.3 nW is achieved for a harvester with a  $16 \text{ cm}^2$  large IXPP film within a Helmholtz resonator, which features a resonance frequency of 900 Hz, with an optimized load resistance of 962 k $\Omega$  under an input SPL of 100 dB. In comparison to acoustic energy harvesters based on ferroelectric polymer polyvinylidene fluoride cantilever beams, our devices have much higher output power density under the same conditions and much broader bandwidth. Theoretical analysis and numerical simulations are performed to confirm the experimental results. Moreover, the output power of the IXPP acoustic energy harvesters can be further improved by increasing the active area of the piezoelectret films.

Keywords: acoustic energy harvesting, piezoelectrets, cross-linked polypropylene

(Some figures may appear in colour only in the online journal)

<sup>5</sup> Authors to whom any correspondence should be addressed.



Original content from this work may be used under the terms of the [Creative Commons Attribution 3.0 licence](https://creativecommons.org/licenses/by/3.0/). Any further distribution of this work must maintain attribution to the author(s) and the title of the work, journal citation and DOI.

## 1. Introduction

In the past decades, energy harvesting from environmental sources, such as sunlight, heat, and mechanical energies, has raised great research interests [1–9]. As regards the mechanical

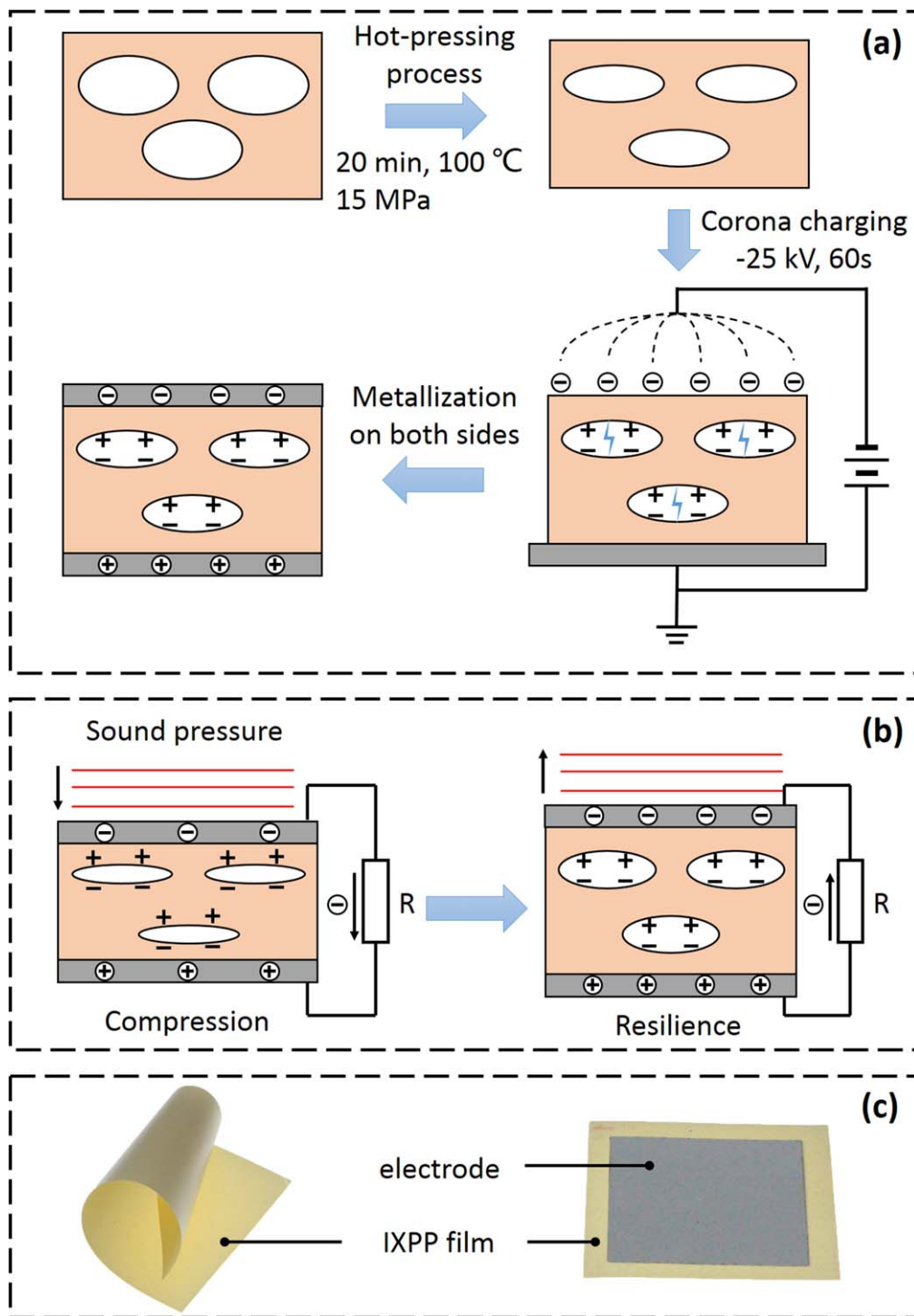


**Figure 1.** Schematic views of (a) the preparation process of IXPP piezoelectret films, (b) the working principle of IXPP piezoelectret devices, and (c) the photographs of IXPP piezoelectret films.

energy, researchers usually focus on scavenging the low-frequency kinetic and/or vibration energy. However, there are several other environmental energy sources that have been less investigated. One example of these neglected energies is acoustic energy, a clean, ubiquitous, and sustainable source in both domestic and industrial environments.

In recent years, a few efforts have been expended on harvesting acoustic energy available in our daily life. Different transduction mechanisms for acoustic energy harvesting have

been proposed and acoustic energy harvesters based on artificial materials and structures have been reported [9–22]. As for piezoelectric acoustic energy harvesting, Horowitz *et al* [11] firstly introduced an electromechanical Helmholtz resonator with piezoelectric diaphragm as an acoustic energy harvesting device. Liu *et al* [12] developed a Helmholtz resonator which converted the acoustic energy to electrical one by bending a piezoelectric back plate in the cavity. After that, Li *et al* [13] proposed a quarter wavelength tube resonator to harvest low-frequency

**Table 1.** The properties of IXPP piezoelectret films.

Material properties	IXPP
Quasi-static $d_{33}$ coefficient	500 pC N <sup>-1</sup>
Relative permittivity $\epsilon_{33}$	1.8
FoM ( $d_{33} \cdot g_{33}$ )	19 GPa <sup>-1</sup>
Young's modulus $Y_3$	1.2 MPa
Density $\rho$	550 kg m <sup>-3</sup>
Electromechanical coupling coefficient $k_t$ [29]	0.08

acoustic energy. Apart from these devices, polyvinylidene fluoride (PVDF) [14, 15], phononic crystal [15, 16], acoustic metamaterials or metasurface [17–19], and broadband gradient-index lens [20] were also applied in acoustic energy harvesting.

In parallel to the progress of harvester design, there is always an interest in new flexible piezoelectric materials. Such a new kind of piezoelectric polymer material, namely piezoelectrets or ferroelectrets [23, 24], has been applied in vibration energy harvesters recently [25–29]. Piezoelectrets are piezoelectric polymer electret foams with oriented ‘macro-dipoles’, which exhibit a strong piezoelectric effect. One of the most promising piezoelectret materials is irradiated cross-linked polypropylene (IXPP), a biocompatible and environmentally friendly plastic polymer [30]. Indeed the IXPP piezoelectret films, as shown in our prior work, feature a figure of merit ( $d_{33} \cdot g_{33}$ , FoM) of 11.2 GPa<sup>-1</sup> [29], being much larger than that of PVDF (0.003 GPa<sup>-1</sup> [31]), and a flat response in the audio range [32], and thus, are appropriate for broadband acoustic energy harvesting. The low acoustic impedance of 0.03 MRayl [32] of IXPP films also suggests an advantage on transferring acoustic energy in air without any matching layers. Moreover, simple structure, flexibility and low cost are also great strengths of IXPP piezoelectret films.

In this work, IXPP piezoelectret films were adopted as a transduction material to convert the acoustic energy into electrical energy in a simple circuit for the first time. A Helmholtz resonator was employed to amplify the incident sound pressure in a prototype device for low-frequency acoustic energy harvesting.

The paper is organized as follows. A brief introduction to the topic of the IXPP piezoelectret is given in the beginning, which is followed by a theoretical analysis of output power of the IXPP piezoelectret energy harvesters. After that, the IXPP acoustic energy harvesters for ultrasonic and low-frequency energy harvesting are reported. Finally, several approaches are discussed to improve the output power of the IXPP piezoelectret film based acoustic energy harvester.

## 2. IXPP piezoelectrets for acoustic energy harvesting

### 2.1. Preparation process

Figure 1(a) shows a schematic view of the preparation process of the IXPP piezoelectret films. There are three main steps in this process. In the first step, i.e. the hot-pressing process [33],

IXPP foam sheets (provided by Shanghai Bozhi Material Co., Ltd) were sandwiched between two metal plates and then pressed under 15 MPa at 100 °C for 20 min, so as to modify the microstructure in the IXPP foam sheets. As a result, Young's modulus of these films in the thickness direction is reduced and their charging capability is enhanced. The second step is the polarization, in which the corona charging of the IXPP films was performed with a needle voltage of –25 kV (without a grid) to render them piezoelectric. In the next step, aluminum layers were evaporated on both sides of the samples with a thickness of about 100 nm. The final IXPP piezoelectret device performs similarly as a common piezoelectric disk, and its working principles are shown in figure 1(b). Photographs of prepared IXPP piezoelectret films are also presented in figure 1(c).

### 2.2. Material properties of IXPP piezoelectrets

For the purpose of analyzing and simulating the performance of IXPP piezoelectret films, several electromechanical properties of such films are experimentally determined.

The quasi-static piezoelectric  $d_{33}$  coefficient of the IXPP samples was measured via the direct piezoelectric effect [34, 35]. In this measurement, a weight was manually removed from the test piezoelectret and the charge generated on the electrodes over 10 s was recorded by using an electrometer (Keithley 6514).

The capacitance  $C$ , Young's modulus in the thickness direction  $Y_3$ , relative permittivity  $\epsilon_{33}$ , and anti-resonance frequency  $f_a$  of the samples were determined from the dielectric resonance spectra, which were measured by a high-precision impedance analyzer (Agilent 4294 A) [29, 36]. The area, thickness, and density of the IXPP films were obtained by measuring and weighing the samples directly.

IXPP piezoelectret films prepared in this study feature an active area of 16 cm<sup>2</sup> and a thickness of 140  $\mu$ m. A summary of the material properties of the IXPP piezoelectret films is listed in table 1. Among these properties, the FoM of IXPP films has been determined to be equal to 19 GPa<sup>-1</sup>, being obviously higher than its counterpart evaluated in former study [29], because of the enlarged piezoelectric coefficient  $d_{33}$  of the IXPP sample in this study; more importantly, the FoM here is dramatically (about 3 orders of magnitude) larger than the one of PVDF piezoelectric polymer (0.003 GPa<sup>-1</sup> [31]), which provides great benefits for harvesting acoustic energy.

## 3. Analysis of output power of IXPP energy harvester

The output power  $P_{\text{out}}$  of an IXPP film energy harvester at angular frequency  $\omega$  and load resistance  $R_l$  is given by [37, 38]

$$P_{\text{out}} = \frac{\left(m_s + \frac{1}{3}m_f\right)^2 d_{33}^2 a^2 R_l \omega^2}{\left[\left(\frac{\omega^2}{\omega_f^2} - 1\right)^2 + 4\zeta_m^2 \left(\frac{\omega}{\omega_f}\right)^2\right] [1 + (R_l C \omega)^2]}, \quad (1)$$

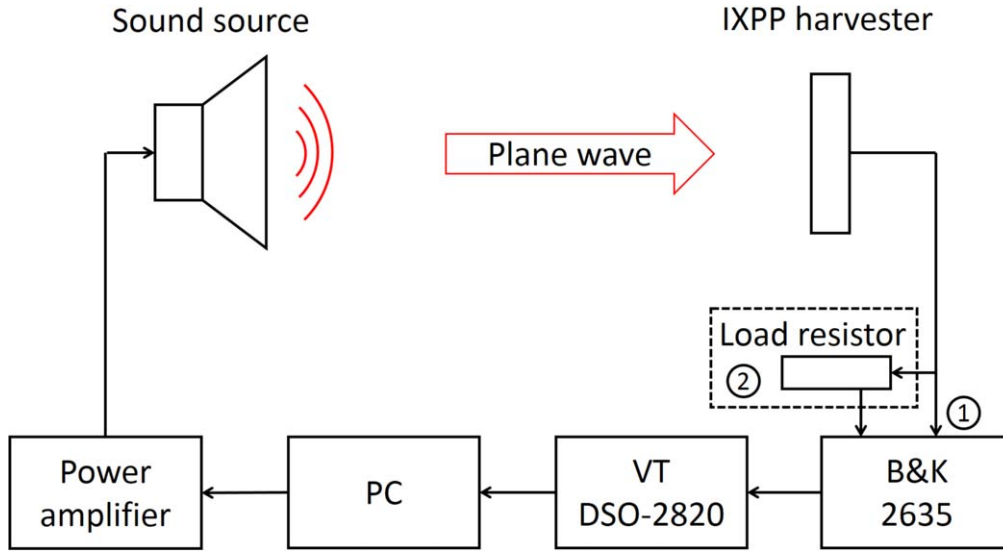


**Figure 2.** Experimental configuration of measurements for output power of IXPP acoustic energy harvesters. ① is for measurement of short-circuit charge of the energy harvester, ② is for measurement of charge flowing through load resistance  $R_l$ .

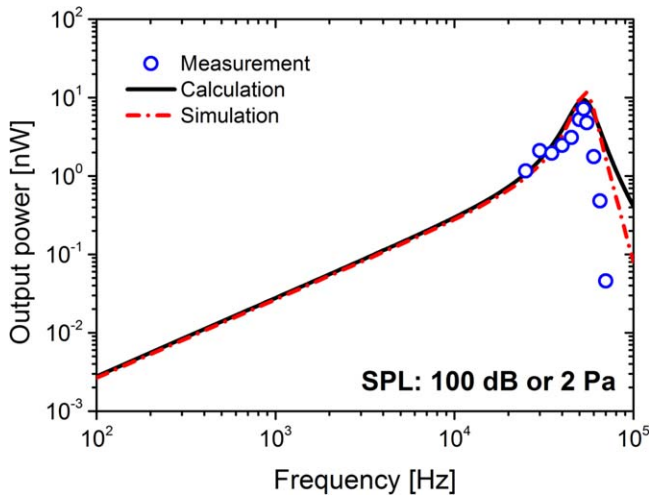


**Figure 3.** Measured, calculated and simulated optimal output power of an IXPP film harvester at an input SPL of 100 dB (2 Pa). The clamped IXPP film harvester has a square shape with an active area of  $16 \text{ cm}^2$ , a quasi-static  $d_{33}$  coefficient of approximately  $400 \text{ pC N}^{-1}$ , and a capacitance of  $185 \text{ pF}$ .

where

$$\omega_f = \sqrt{\frac{Y_3 A}{t \left( m_s + \frac{1}{3} m_f \right)}} \quad (2)$$

is the resonance angular frequency of the IXPP film sample,  $a$  is the input acceleration,  $\zeta_m$  is the damping ratio,  $m_s$  is the seismic mass;  $\frac{1}{3} m_f$  and  $A$  represent the effective mass and area of the piezoelectret film, respectively; and  $C$  is the sum of sample and parasitic capacitances. The damping ratio  $\zeta_m$  depends on a number of parameters and is determined from the measurements of the charge sensitivity of piezoelectret energy harvesters in general.

When no seismic mass is involved ( $m_s = 0$ ), for a harmonic excitation, the input acceleration  $a$  is given by

$$a = \frac{F}{\frac{1}{3} m_f} = \frac{pA}{\frac{1}{3} m_f}, \quad (3)$$

where  $p$  indicates the actual sound pressure applied on the IXPP film.

The maximum output power may be harvested at the resonance frequency  $\omega_f$  if a terminal load resistance of  $R_l = 1/\omega_f C$  is chosen. In this case the maximum harvested power  $P_m$  is written as [37]

$$P_m = \frac{p^2 A^2 d_{33}^2 \omega_f}{8 \zeta_m^2 C}. \quad (4)$$

When the working frequency  $\omega$  is much smaller than the resonance  $\omega_f$  of the IXPP film sample itself ( $\omega \ll \omega_f$ ), and a terminal load resistance  $R_l = 1/\omega C$  is selected, the optimal output  $P_{\text{out}}$  of the IXPP harvester, given in equation (1), can be simplified as

$$P_{\text{opt}} = \frac{1}{2} d_{33}^2 p^2 A^2 R_l \omega^2 = \frac{1}{2C} d_{33}^2 p^2 A^2 \omega. \quad (5)$$

Neglecting the parasitic capacitance, one has [34]

$$\frac{d_{33}}{C} = g_{33} \frac{t}{A}, \quad (6)$$

where  $t$  is the total thickness of the IXPP piezoelectret film. Thus, equations (4) and (5) can be written as

$$P_m = \frac{p^2 A d_{33} g_{33} \omega_f^2 t}{8 \zeta_m^2} \quad (7)$$

and

$$P_{\text{opt}} = \frac{1}{2} d_{33} g_{33} p^2 A \omega t. \quad (8)$$

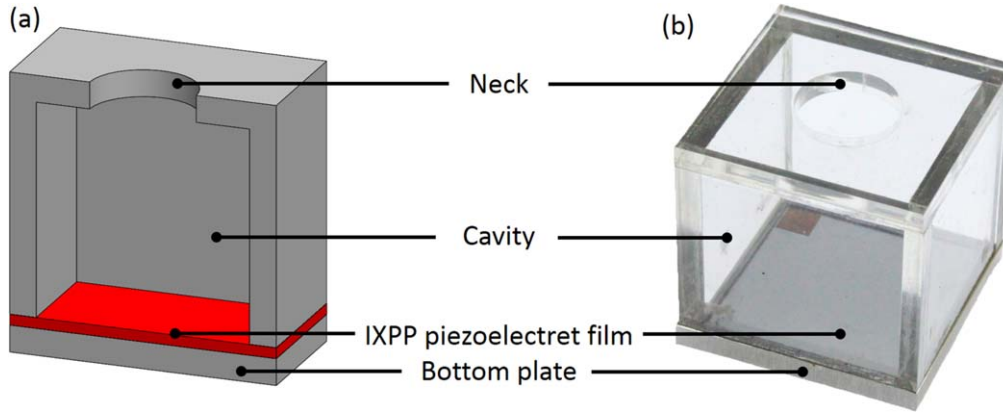


**Figure 4.** (a) Cross-sectional view and (b) optical image of a low-frequency IXPP piezoelectret film acoustic energy harvester. This harvester is made of a Helmholtz resonator and an IXPP piezoelectret film.

These equations imply that the product  $d_{33} \cdot g_{33}$ , which is known as the FoM for piezoelectret transmit-receive systems, is also the FoM for the piezoelectret energy harvester. This is also the reason why the IXPP piezoelectret featuring a large FoM serves as a suitable candidate for the energy harvester.

#### 4. Acoustic energy harvesting with IXPP piezoelectret films

##### 4.1. Experimental setup

Figure 2 shows the experimental setup for acoustic energy harvesting with IXPP films both in the audio and ultrasonic ranges. A commercial loudspeaker was utilized for the audio range test, and an IXPP piezoelectret film based speaker was fabricated and used for the ultrasonic range experiment. In both cases, the sound source was connected to a power amplifier (DSPPA MP200P III/PINTEK HA-800) which magnified the electrical signals sent from the personal computer. In return, sound waves emitted from the speakers impinge normally on the surface of IXPP acoustic energy harvesters located in the far field, exciting the IXPP films into vibration. A charge amplifier (B&K-2635) was employed to convert the generated charge into voltage signal, whereas a multi-function virtual instrument software (MI 3.7, Virtins Technology, type DSO-2820) was implemented in the computer for signal generation, recording, and analysis. The sound pressure of the incident acoustic waves was measured by a calibrated microphone (B&K-4138). No seismic mass was applied on the IXPP samples in this paper since the IXPP samples have low acoustic impedance and the application of a seismic mass would reflect most of the incident acoustic energy.

The optimized output power  $P_{\text{opt}}$  of an IXPP energy harvester at frequency  $\omega$  can be determined from either the measurement of the charge  $Q_R$  through the optimized load resistance  $R_{\text{opt}} = 1/\omega C$ , or from the short-circuit charge  $Q_{\text{sc}}$  at the resonance frequency [39], as given by

$$P_{\text{opt}} = R_{\text{opt}} I^2 = R_{\text{opt}} \omega^2 Q_R^2 = \frac{1}{2C} \omega Q_{\text{sc}}^2, \quad (9)$$

with the relationship that  $Q_{\text{sc}} = Q_R/\sqrt{2}$  for the optimized resistance. In this paper, both methods were utilized to determine the output power generated from IXPP acoustic energy harvesters.

##### 4.2. Acoustic energy harvesting with IXPP film harvester

As pointed out in section 3, the maximum output power of an IXPP film harvester may be achieved at its resonance frequency. Figure 3 illustrates the optimal output power of an IXPP film acoustic energy harvester obtained from measurement (circle markers), theoretical calculation with equation (1) (solid line), and numerical simulation (dashed line), under an applied sound pressure level (SPL) of 100 dB (or 2 Pa). Here, numerical simulations are conducted with a commercial software, COMSOL Multiphysics. Material properties of the IXPP films described in section 2.2 are adopted for the simulations. The IXPP harvesters used here have an active area of  $16 \text{ cm}^2$ , a capacitance of 185 pF, and a quasi-static  $d_{33}$  coefficient of  $400 \text{ pC N}^{-1}$ . In addition, the IXPP film is fixed on one side on a PMMA plate with double sided adhesive tape during this experiment. Thus, only the other side of the IXPP film is excited to vibrations by the sound waves. This is different from piezoelectric ceramics. The PMMA plate is also used to support the flexible IXPP films.

As shown in figure 3, the experimental output power of this IXPP film harvester increases all the more below the resonance frequency, corresponding well to the theoretical results derived from equation (1) and the numerical simulations. At its resonance frequency of around 53 kHz, a maximum output power of around 7.2 nW (a power density of  $4.5 \times 10^{-4} \mu\text{W cm}^{-2}$ ) is obtained for this IXPP film harvester with an optimal load resistance of 16.3 k $\Omega$ . Above the resonance frequency, the output power decreases dramatically, as expected. Due to the limit of the device and the expected low power of electrical energy harvested at low frequencies, the output power of this IXPP film harvester is only experimentally measured in the ultrasonic range.

The maximum output power of the IXPP film harvester obtained from the calculation and the numerical simulation,

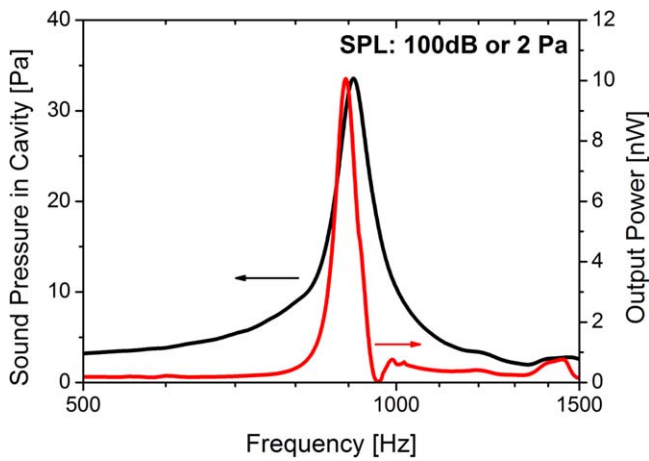


**Figure 5.** Measured sound pressure in the cavity (black) and output power (red) of the low-frequency IXPP acoustic energy harvester acquired from the short-circuit charge obtained at an input SPL of 100 dB (2 Pa). The IXPP harvester has a square shape with an active area of 16 cm<sup>2</sup>, a quasi-static  $d_{33}$  coefficient of approximately 550 pC N<sup>-1</sup>, a capacitance of 185 pF, and an optimal load resistance of 962 k $\Omega$ .

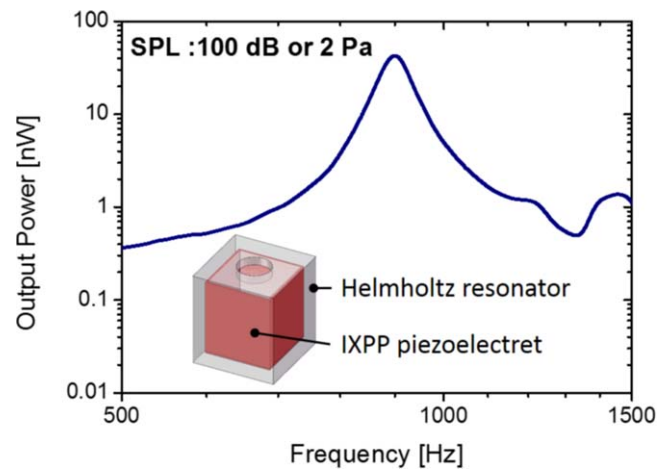


**Figure 7.** Schematic view (inset) and generated output power of an acoustic energy harvester consisting of a Helmholtz resonator with five IXPP films at an input SPL of 100 dB (2 Pa). The IXPP films have a square shape with total active area of 80 cm<sup>2</sup>, a quasi-static  $d_{33}$  coefficient of 550 pC N<sup>-1</sup>, and an optimal load resistance of 280 k $\Omega$ .

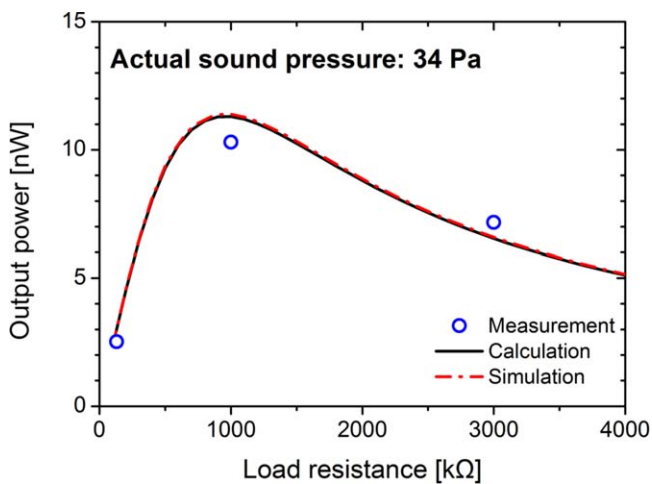


**Figure 6.** Measurement, calculation and simulation results of output power as a function of load resistance  $R_l$  for a low-frequency IXPP film acoustic energy harvester.

using the above parameter values and a mechanical damping ratio of 0.23 determined from experiment, are 9.4 and 11.6 nW, respectively, close to that from the measurement. The quality factor for the resonant power peak is 2.5. According to equation (2), a resonance frequency of 55 kHz is achieved for these IXPP films with a Young's modulus of 0.9 MPa, a thickness of 180  $\mu$ m, an active area of 10 cm<sup>2</sup>, and a total film mass of 0.2 g. This calculated resonance frequency of the IXPP samples is close to the measured one and lower than that mentioned in the literature [32]. This is due to the fact that the resonance frequency for a clamped sample is half that of a free-standing sample [40], which is about 120 kHz [32].

#### 4.3. Low-frequency acoustic energy harvesting

It is also of interest to develop IXPP film harvesters for scavenging low-frequency acoustic energy at low frequencies when considering that most of the sound sources available in daily life contain predominantly low-frequency components. These components are also less attenuated by air absorption in comparison to high frequency sound [38]. Although the IXPP film harvester achieves its maximum output at its resonance, the large FoM of IXPP piezoelectret films also guarantees these films to be promising candidates for low-frequency acoustic energy harvesting.

Here, in order to harvest low-frequency acoustic energy more efficiently, a Helmholtz resonator made of 5 mm thick PMMA was used. This widely used tool for sound augmentation and noise attenuation was introduced here to amplify the incident sound pressure so as to increase the output power of the IXPP acoustic energy harvester. The low-frequency IXPP acoustic energy harvesters were prepared in such a way that the IXPP piezoelectret films were attached to the bottom plate of the Helmholtz resonators with double sided adhesive tape. The cross-sectional view and optical image of a low-frequency IXPP harvester are presented in figure 4. In this experiment, the IXPP films are fixed on a thick PMMA bottom plate. Due to the flat frequency response of the IXPP film at low frequencies, such a device has a maximum output at a frequency close to that of the Helmholtz resonator. Also, because of the hardness of the PMMA plate, this setup yields the well-known buildup of sound pressure on its front and thus an additional increase of the electrical output. As an alternative, a thin flexible membrane could be used to mount the IXPP films in the low-frequency acoustic energy harvesters [41]. This, however, makes the whole device a more complicated coupled system, whose output depends on its mounting and on the geometric dimensions, design, and materials. Corresponding studies are under way and the

performance of IXPP acoustic energy harvesters utilizing such flexible membranes will be discussed in the future.

Figure 5 presents the measured sound pressure in the cavity (black line) and the output power of the low-frequency IXPP acoustic energy harvester (red line) obtained experimentally under an input SPL of 100 dB. The output power of the harvester features a peak value close to the resonance of the used Helmholtz resonator (900 Hz), as expected. According to this figure, a maximum output power of 10.3 nW, a power density of  $6.4 \times 10^{-4} \mu\text{W cm}^{-2}$ , and a quality factor of 17.9 are achieved for this harvester with equation (9) at the frequency of 900 Hz with an optimized load resistance of 962 k $\Omega$ . The amplification of sound pressure in the cavity for this device is only 17, being smaller than those of Helmholtz resonators made of different materials, i.e. steel and aluminum [14, 22, 42]. This is may be due to the considerable damping effect of PMMA material. High quality factor Helmholtz resonators made of alternative hard materials for IXPP film acoustic energy harvesting will be discussed in a future study.

The optimized output power of the IXPP energy harvester can also be calculated by using equation (5) or (8) from the properties of the IXPP sample and the acoustic characteristics of the Helmholtz resonator. The resulting optimized output power derived from equation (5) is equal to 13 nW, being close to the measured value (10.3 nW). The discrepancy between these two values is probably associated with the dynamic  $d_{33}$  of the IXPP piezoelectret, which is smaller than the quasi-static counterpart but is applicable for the measured value. Besides, the acoustic pressure sensitivity of such an IXPP sample  $M_p$ , defined by  $M_p = V_0/p$ , where  $V_0$  is the generated open-circuit voltage, is evaluated as 4 mV Pa $^{-1}$ . This is almost the same as the value 3.8 mV Pa $^{-1}$  reported in former study [32].

A comparison with an acoustic energy harvester using a single-layer PVDF cantilever beam [14] with a maximum output power of  $\sim 0.033 \mu\text{W}$  ( $7.3 \times 10^{-3} \mu\text{W cm}^{-2}$ ), described in the literature, is of interest. The low-frequency IXPP acoustic energy harvester under the same conditions, i.e. a resonance of the Helmholtz resonator of 865 Hz and an actual acoustic pressure of  $\sim 400$  Pa in the cavity is expected to have a power density of  $0.1 \mu\text{W cm}^{-2}$ , more than 10 times that of the above PVDF beam cantilever based acoustic energy harvester. It is worth noting that the output of the PVDF harvester has to match the resonance of the Helmholtz resonator and the PVDF cantilever so as to achieve a high output power, while the IXPP film based harvesters have a simpler structure because of that IXPP piezoelectret films have a flat response in the audio range, ensuring the compatibility with different acoustic resonators.

Investigations on the output power of the IXPP film harvesters using different load resistances  $R_l$  were also carried out in this study. Figure 6 shows the measured (circle markers), calculated (solid line) and simulated (dashed line) output power of the IXPP acoustic energy harvester as a function of load resistance  $R_l$  under an applied sound pressure of 34 Pa. The load resistances used in this measurement are 130 k $\Omega$ , 1 M $\Omega$ , and 3 M $\Omega$ , respectively. The simulated output

power of the IXPP harvester is close to the one calculated from equation (1); further, the experimental result is in good agreement with the simulation and analytical results as well. In addition, the maximum output power of this IXPP harvester is close to 10 nW with a load resistance of 1 M $\Omega$  at 900 Hz, almost the same as its counterpart of 10.3 nW in figure 5. This corresponds quite well to equation (9).

#### 4.4. Enhancements for IXPP acoustic energy harvester

For the sake of improving the energy level of these IXPP acoustic energy harvesters, several approaches are proposed and implemented. Among these effective approaches, one of them is to increase the active area of the IXPP films. For example, for the low-frequency harvesters, the active area in such an IXPP acoustic energy harvester prototype can be multiplied by attaching more IXPP films to the inner walls of the Helmholtz cavity. To this end, a low-frequency IXPP harvester using a Helmholtz resonator with five IXPP film samples attached on its five inner walls (except the top wall) is prepared. Figure 7 shows the total output power of the prepared harvester with all the five IXPP film samples in electrical parallel but mechanical series, featuring a peak power of 43 nW at the resonance frequency of 900 Hz with the optimized load resistance of 280 k $\Omega$ . This is almost five times the power compared to the device having just a single-wall covered with IXPP, as used in figure 6 at the same frequency.

Another way to enhance the efficiency of an IXPP acoustic energy harvester consists in using a stacked or/and folded structure of IXPP films. As compared with the single-layer piezoelectret film, the stacked and folded piezoelectret films have a larger  $d_{33}$  response, and therefore a larger receiving sensitivity in the application as microphones [43], and a larger output power in vibration-based energy harvesters [37]. However, one has to consider the fact that the resonance frequency of stacked and folded IXPP piezoelectret films may be influenced by the number of layers and/or the glue utilized between layers. Results on IXPP acoustic energy harvesters using stacked and folded IXPP piezoelectret films will be discussed in a future study.

## 5. Conclusions




We have demonstrated acoustic energy harvesters using IXPP piezoelectret films with large FoM. A maximum output power of 7.2 nW is obtained for an IXPP film acoustic energy harvester at its resonance frequency of 53 kHz, an optimal load resistance of 16.3 k $\Omega$  and an input SPL of 100 dB. The flat response in the audio range and large FoM of IXPP films also make the IXPP film suitable for harvesting low-frequency acoustic energy. Helmholtz resonators were introduced to improve the efficiency of IXPP acoustic energy harvesters. An output power of 10.3 nW is achieved for an IXPP harvester within a Helmholtz resonator at a frequency of 900 Hz for an input SPL of 100 dB with an optimized load resistance of 962 k $\Omega$ . Theoretical results as well as numerical

simulations show good agreement with the experimental data. When compared with acoustic energy harvesters using PVDF cantilever beams, the IXPP acoustic energy harvesters produce a higher power density under the same conditions, yet featuring a simpler structure. The output power of the IXPP acoustic energy harvesters can be further improved by increasing the active area of the IXPP piezoelectret films. Moreover, the low cost, low acoustic impedance, flexibility, biocompatibility and environmental friendliness are strengths of IXPP piezoelectrets. Such films are thus expected to find use in acoustic energy harvesting in the future.

## Acknowledgments

Financial support from the Natural Science Foundation of China (Grants No. NFSC 61761136004, 11602174 and 11374232), the Fundamental Research Funds for the Central Universities (Grant No. 2016KJ008), and funding by the Deutsche Forschungsgemeinschaft (DFG, German Research Foundation, Projektnummer 392020380 and KU3498/1) is gratefully acknowledged.

## ORCID iDs

Yuan Xue  <https://orcid.org/0000-0001-9005-4982>  
 Jinfeng Zhao  <https://orcid.org/0000-0003-1751-6858>  
 Gerhard M Sessler  <https://orcid.org/0000-0003-1169-6907>

## References

- [1] Priya S and Inman D J 2009 *Energy Harvesting Technologies* (Berlin: Springer)
- [2] Elvin N and Erturk A 2012 *Advances in Energy Harvesting Methods* (Berlin: Springer)
- [3] Khaligh A and Onar O C 2009 *Energy Harvesting: Solar, Wind, and Ocean Energy Conversion Systems* (Boca Raton: CPC Press)
- [4] Beeby S and White N 2010 *Energy Harvesting for Autonomous Systems* (Boston, MA: Artech House)
- [5] Briand D, Yeatman E and Roundy S 2015 *Micro Energy Harvesting* (New York: Wiley)
- [6] Mitcheson P D, Yeatman E M, Rao G K, Holmes A S and Green T C 2008 *Proc. IEEE* **96** 1457–86
- [7] Erturk A and Inman D J 2011 *Piezoelectric Energy Harvesting* (New York: Wiley)
- [8] Ilyas M A 2018 *Piezoelectric Energy Harvesting: Methods, Progress, and Challenges* (New York: Momentum Press)
- [9] Khan F U and Izhar 2015 *J. Micromech. Microeng.* **25** 023001
- [10] Pillai M A and Deenadayalan E 2014 *Int. J. Precis. Eng. Manuf.* **15** 949–65
- [11] Horowitz S B, Sheplak M, Cattafesta L N and Nishida T 2006 *J. Micromech. Microeng.* **16** S174–81
- [12] Liu F, Phipps A, Horowitz S, Ngo K, Cattafesta L, Nishida T and Sheplak M 2008 *J. Acoust. Soc. Am.* **123** 1983–90
- [13] Li B, You J H and Kim Y J 2013 *Smart Mater. Struct.* **22** 055013
- [14] Noh S, Lee H and Choi B 2013 *Int. J. Precis. Eng. Manuf.* **14** 1629–35
- [15] Wu L Y, Chen L W and Liu C M 2009 *Appl. Phys. Lett.* **95** 013506
- [16] Yang A, Li P, Wen Y, Lu C, Peng X, Zhang J and He W 2013 *Appl. Phys. Express* **6** 127101
- [17] Liu G, Peng Y, Liu M, Zou X and Cheng J 2018 *Appl. Phys. Lett.* **113** 153503
- [18] Qi S, Oudich M, Li Y and Assouar B 2016 *Appl. Phys. Lett.* **108** 263501
- [19] Assouar B, Qi S and Li Y 2017 Quantum Sensing and Nano Electronics and Photonics *Proc. SPIE 10111* **XIV** 101112B
- [20] Tol S, Degertekin F L and Erturk A 2017 *Appl. Phys. Lett.* **111** 013503
- [21] Yuan M, Cao Z, Luo J and Pang Z 2018 *AIP Adv.* **8** 085012
- [22] Yuan M, Cao Z, Luo J, Zhang J and Chang C 2017 *Sensors Actuators A* **264** 84–9
- [23] Bauer S, Gerhard-Multhaupt R and Sessler G M 2004 *Phys. Today* **57** 37–43
- [24] Leikkala J, Poramo R, Nyholm K and Kaikkonen T 1996 *Med. Biol. Eng. Comput.* **34** 67–8
- [25] Anton S R, Farinholt K M and Erturk A 2014 *J. Intell. Mater. Syst. Struct.* **25** 1681–92
- [26] Pondrom P, Hillenbrand J, Sessler G M, Bös J and Melz T 2015 *IEEE Trans. Dielectr. Electr. Insul.* **22** 1470–6
- [27] Feng Y, Hagiwara K, Iguchi Y and Suzuki Y 2012 *Appl. Phys. Lett.* **100** 262901
- [28] Luo Z, Zhu D and Beeby S P 2015 *J. Phys.: Conf. Ser.* **660** 012118
- [29] Zhang X, Wu L and Sessler G M 2015 *AIP Adv.* **5** 077185
- [30] Shi Q, Zhao J, Stagnaro P, Yang H, Luan S and Yin J 2012 *J. Appl. Polym. Sci.* **126** 929–38
- [31] Mrlík M, Leadenham S, Almaadeed M A and Erturk A 2016 Active and Passive Smart Structures and Integrated Systems *Proc. SPIE* **9799** 979923
- [32] Xue Y, Zhang X, Zheng J, Liu T and Zhu B 2018 *IEEE Trans. Dielectr. Electr. Insul.* **25** 228–34
- [33] Zhang X, Huang J, Chen J, Wan Z, Wang S and Xia Z 2007 *Appl. Phys. Lett.* **91** 182901
- [34] Hillenbrand J and Sessler G M 2000 *IEEE Trans. Dielectr. Electr. Insul.* **7** 537–42
- [35] Zhang X, Zhang X, Sessler G M and Gong X 2014 *J. Phys. D: Appl. Phys.* **47** 015501
- [36] Zhang X, Sessler G M, Xue Y and Ma X 2016 *J. Phys. D: Appl. Phys.* **49** 205502
- [37] Pondrom P, Hillenbrand J, Sessler G M, Bös J and Melz T 2014 *Appl. Phys. Lett.* **104** 172901
- [38] Kinsler L E, Frey A R and Bennett G S 1982 *Fundamentals of Acoustics* (New York: Wiley)
- [39] Hillenbrand J, Pondrom P and Sessler G M 2015 *Appl. Phys. Lett.* **106** 183902
- [40] Fang P, Holländer L, Wirges W and Gerhard R 2012 *Meas. Sci. Technol.* **23** 035604
- [41] Horowitz S B, Nishida T, Cattafesta L N and Sheplak M 2002 *Int. J. Aeroacoust.* **1** 183–205
- [42] Yang A, Li P, Wen Y, Lu C, Peng X, He W, Zhang J, Wang D and Yang F 2014 *Rev. Sci. Instrum.* **85** 066103
- [43] Hillenbrand J and Sessler G M 2004 *J. Acoust. Soc. Am.* **116** 3267